Development of a Far-Red to Near-Infrared Fluorescence Probe for Calcium Ion and its Application to Multicolor Neuronal Imaging

Takahiro Egawa, Kenjiro Hanaoka, Yuichiro Koide, Sakiko Ujita, Naoya Takahashi, Yuji Ikegaya, Norio Matsuki, Takuya Terai, Tasuku Ueno, Toru Komatsu, and Tetsuo Nagano*

Graduate School of Pharmaceutical Sciences, The University of Tokyo, 7-3-1 Hongo, Bunkyo-ku, Tokyo 113-0033, Japan

S Supporting Information

ABSTRACT: To improve optical imaging of Ca^{2+} and to make available a distinct color window for multicolor imaging, we designed and synthesized CaSiR-1, a far-red to near-infrared fluorescence probe for Ca^{2+}, using Si-rhodamine (SiR) as the fluorophore and the well-known Ca^{2+} chelator BAPTA. This wavelength region is advantageous, affording higher tissue penetration, lower background autofluorescence, and lower phototoxicity in comparison with the UV to visible range. CaSiR-1 has a high fluorescence off/on ratio of over 1000. We demonstrate its usefulness for multicolor fluorescence imaging of action potentials (visualized as increases in intracellular Ca^{2+}) in brain slices loaded with sulforhodamine 101 (red color; specific for astrocytes) that were prepared from transgenic mice in which some neurons expressed green fluorescent protein.

Calcium ion (Ca^{2+}) is a pivotal second messenger inside cells,[1] and visualization of the intracellular dynamics of Ca^{2+} has yielded substantial biological knowledge.[2−8] To understand information processing by neurons, optical imaging of neuronal action potentials in terms of somatic Ca^{2+} increase is currently being used in the field of neuroscience.[9−14] Although electro-physiological recording techniques are superior in terms of temporal resolution, fluorescence imaging of Ca^{2+} provides a unique opportunity to analyze the profile of multineuronal activities because bulk-loading methods using acetoxymethyl (AM) ester derivatives of Ca^{2+} probes have been established for simultaneous monitoring of more than 1000 individual neurons,[15] which is impossible with other methods such as patch-clamp recording and functional magnetic resonance imaging.[16−21]

Since the first introduction of a fluorescence probe for Ca^{2+}, many probes with various characteristics have been developed to meet the demands of researchers.[22] UV to visible fluorescence probes such as Fura-2[2] have been most widely utilized in almost all research areas; however, far-red to near-infrared (NIR) fluorescence probes are expected to be superior because the light in this wavelength region shows greater tissue penetration, has less overlap with the spectrum of background autofluorescence, and exhibits less phototoxicity.[23] Furthermore, far-red to NIR fluorescence is likely to be separable from the fluorescence windows of other fluorescence indicators and markers, including genetically expressed fluorescent proteins,[22] and thus has potential for multicolor imaging. Therefore, we sought to develop a novel far-red to NIR fluorescence probe for Ca^{2+} that would be suitable for investigating intracellular Ca^{2+} dynamics and for multicolor imaging.

This is a challenging task because almost all far-red to NIR fluorescence dyes, such as cyanine dyes, have relatively high-lying highest occupied molecular orbital (HOMO) energy levels, which means that fluorescence of these dyes is unlikely to be quenched efficiently via the photoinduced electron transfer (PeT) mechanism,[24] which is the fluorescence-controlling mechanism generally used for off/on-type Ca^{2+} probes.[25] As a result, previously reported far-red to NIR fluorescence probes for Ca^{2+} have high background fluorescence and low values of the activation ratio,[25,26] making them inadequate for biological research applications.

We recently reported a unique far-red to NIR fluorophore, Si-rhodamine (SiR),[27,28] so we chose this dye as a scaffold for the development of a novel Ca^{2+} probe. The unique feature of SiR is that it has relatively low-lying lowest unoccupied molecular orbital (LUMO) and HOMO energy levels,[29] and consequently, the PeT threshold of SiR differs greatly from those of other long-wavelength fluorophores. As a Ca^{2+} chelator, we chose the well-known 1,2-bis(o-aminophenoxy)ethane-N,N,N′,N′-tetraacetic acid (BAPTA) moiety. The fluorophore and chelator were coupled via a short linker to afford the new probe, CaSiR-1 (Figure 1a).[3]

First we examined the photophysical properties of CaSiR-1. The fluorescence intensity increased with increasing concentration of free Ca^{2+}, while the absorption spectrum scarcely changed (Figure 1b,c). The fluorescence intensity of 0 μM free Ca^{2+} solution was too small to be distinguished from the baseline, and the maximum activation ratio of the fluorescence intensity (39 μM free Ca^{2+}/0 μM free Ca^{2+}, averaged intensity from 660 to 670 nm) reached 1370. In the design of this probe, we considered that a short distance between SiR and BAPTA would be preferable because a larger separation of the chelator from the fluorophore would be expected to result in a smaller change in PeT efficiency upon chelation or release of Ca^{2+}. To confirm this, we also synthesized another Ca^{2+} indicator (compound **12**; see Scheme 2 in the Supporting Information) in which the two elements are relatively distant, and indeed, it showed a rather small activation ratio (Figures S2−S4 in the Supporting Information). Furthermore, the fluorescence quantum yield of CaSiR-1 was 0.20 in the presence of 39 μM free Ca^{2+}, and the K_d value was 0.58 μM. These values are sufficient for detection of
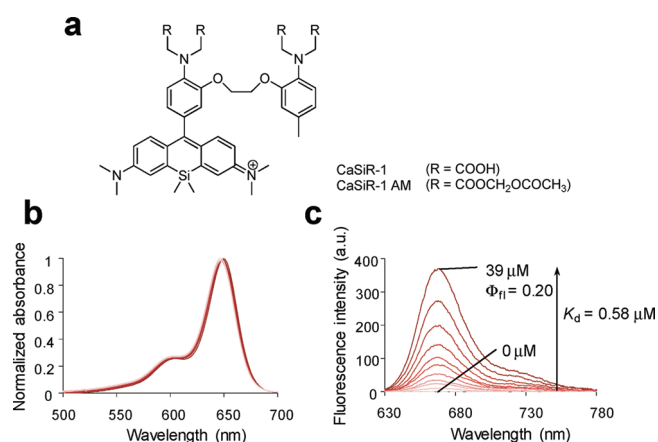
Figure 1. (a) Chemical structures of the novel Ca^{2+} fluorescence probe CaSiR-1 and its cell-permeable derivative CaSiR-1 AM. (b) Absorption and (c) emission spectra of 1 μM CaSiR-1 in the presence of various concentrations of free Ca^{2+} (0, 0.017, 0.038, 0.065, 0.100, 0.150, 0.225, 0.351, 0.602, 1.35, and 39 μM) in 30 mM 3-(N-morpholino)propanesulfonic acid (MOPS) buffer containing 100 mM KCl and 10 mM ethylene glycol tetraacetic acid (EGTA) (pH 7.2) at 22 °C. The excitation wavelength was 620 nm. The fluorescence quantum yield in the presence of 39 μM Ca^{2+} was 0.20. The fluorescence spectrum of the Ca^{2+}-free solution was indistinguishable from the baseline.
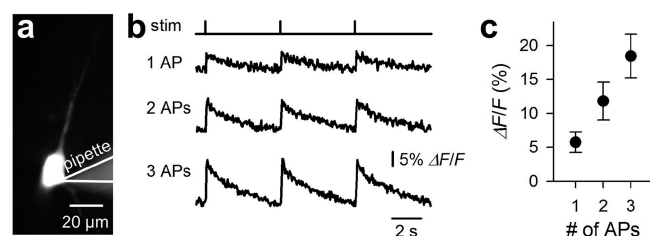

Figure 2. (a) Mouse hippocampal CA1 pyramidal cell loaded with CaSiR-1 through a patch pipet. (b) Action potential (AP)-induced increases in the CaSiR-1 fluorescence intensity of the neuronal cell body. APs were evoked by current injection (stim) into the neuron through a patch-clamp pipet. Each stimulus consisted of 1−3 current pulses, which evoked a burst of 1−3 APs. (c) Increased in the amplitude of the fluorescence change as a function of the number of APs. Error bars: mean ± SD. The frame rate was 20 Hz.

changes in the intracellular Ca^{2+} concentration over the usual range, which is generally on the order of 0.1 μM.

Next, to examine the utility of CaSiR-1, we employed this probe to visualize the action-potential-mediated Ca^{2+} increase in the neuronal cell body. Neurons were loaded with CaSiR-1 through whole-cell recording pipettes (Figure 2a), and action potentials were evoked with brief current injections. Action potentials were detectable as time-dependent fluorescence intensity changes (Figure 2b). Furthermore, the amplitude of the fluorescence change was positively correlated with the number of action potentials, allowing the number of action potentials to be estimated (Figure 2c).

We further synthesized CaSiR-1 AM, the cell-membrane-permeable AM ester of CaSiR-1, for network analyses of neuron populations (Figure 1a). AM ester formation is a widely used method for increasing permeability; although CaSiR-1 itself is almost cell-impermeable because of its high water solubility, CaSiR-1 AM can diffuse across cell membranes. The AM ester is
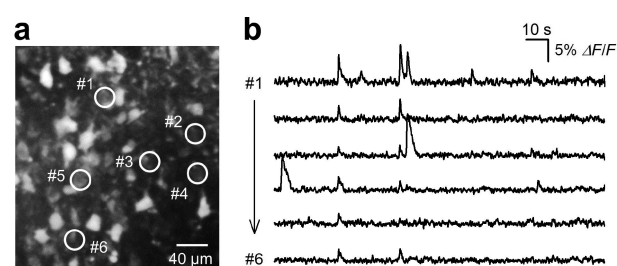
Figure 3. (a) Mouse cerebral cortical neurons loaded with CaSiR-1 AM. (b) Fluorescence traces of individual cells identified in (a). Spontaneous action potentials were visualized in each cell, and some of the activities were synchronized across neurons. The frame rate was 10 Hz.
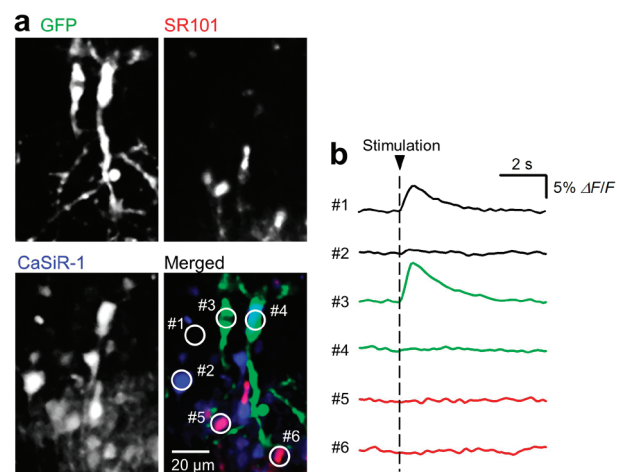
Figure 4. (a) Triple-color imaging and the merged image of an acute hippocampal slice prepared from a Thy1-mGFP mouse. The CA1 pyramidal cell layer, which contains a small fraction of GFP-positive neurons (green) was loaded with CaSiR-1 AM (blue) and sulforhodamine 101 (red), an astrocyte-specific fluorescent marker. (b) Electrical stimulation of Schaffer collateral-induced calcium responses of the cells numbered in (a). The frame rate was 10 Hz.

readily cleaved by intracellular esterase, resulting in intracellular release of the probe in the cell-impermeable form. Thus, high intracellular accumulation can be achieved nearly noninvasively. We bulk-loaded acute cerebral cortex slices with CaSiR-1 AM and observed spontaneous neuronal firing expressed in terms of somatic changes in the CaSiR-1 fluorescence intensity (Figure 3). The simultaneous activation of plural neurons was identifiable (Figure 3b; also see the movie in the Supporting Information), demonstrating synchronous action potentials across neurons, which are thought to play an important role in brain function.

Finally, we examined the potential for use of the fluorescence wavelength region of CaSiR-1 as a new color window for multicolor imaging of Ca^{2+}. Acute brain slices were prepared from transgenic mice in which a fraction of neurons expressed green fluorescent protein (GFP; green color) and loaded with both CaSiR-1 AM and sulforhodamine 101 (SR101, red color), a fluorescent marker specific for astroglial cells (Figure 4).[30] Electrical stimulation was applied to evoke action potentials in a small population of neurons of the CA1 pyramidal cell layer. We succeeded in optically separating the CaSiR-1 signal from the fluorescence of GFP and SR101, allowing us to visualize the neuronal Ca^{2+} dynamics.

In conclusion, we have synthesized CaSiR-1 as the first biologically applicable far-red to NIR fluorescence probe for Ca^{2+}. Some far-red to NIR fluorescence probes have already been reported, but they all have significant drawbacks. For example, Fura Red shows a decrease in its fluorescence intensity in response to increment of free Ca^{2+}, which often makes it difficult to use in biological systems. Moreover, its excitation wavelength lies in a shorter wavelength region (400−500 nm), which, in contrast to the far-red to NIR region, does not offer the advantages of high tissue penetration, low autofluorescence, and low phototoxicity.[23] Other probes show low off/on ratios and in fact are not used in biological research.[25,26] Our results indicate that CaSiR-1 and its AM ester offer great advantages over existing probes for fluorescence imaging of Ca^{2+} in neuronal systems, and we have also confirmed that this probe can be used for multicolor imaging of neuronal action potentials in brain slices. We believe that CaSiR-1 could become the first choice of a fluorescence probe for Ca^{2+} in the far-red to NIR window for optical imaging in wide range of biological areas such as neuroscience.

■ ASSOCIATED CONTENT

ⓢ Supporting Information. Synthesis, experimental details, characterization of CaSiR-1 and another fluorescence probe for Ca^{2+}, complete ref 5, and a movie (AVI) showing the optical imaging of spontaneous neuronal firing in mouse cerebral cortex loaded with CaSiR-1 AM (speeded up by a factor of 10). This material is available free of charge via the Internet at http://pubs.acs.org.

■ AUTHOR INFORMATION

Corresponding Author
tlong@mol.f.u-tokyo.ac.jp

■ ACKNOWLEDGMENT

■ REFERENCES

(1) Clapham, D. E. *Cell* **2007**, *131*, 1047–1058.

(2) Grynkiewicz, G.; Poenie, M.; Tsien, R. Y. *J. Biol. Chem.* **1985**, *260*, 3440–3450.

(3) Minta, A.; Kao, J. P. Y.; Tsien, R. Y. *J. Biol. Chem.* **1989**, *264*, 8171–8178.

(4) Harootunian, A. T.; Kao, J. P. Y.; Paranjape, S.; Tsien, R. Y. *Science* **1991**, *251*, 75–78.

(5) Chambers, J.; et al. *Nature* **1999**, *400*, 261–265.

(6) Micu, I.; Ridsdale, A.; Zhang, L.; Woulfe, J.; McClintock, J.; Brantner, C. A.; Andrews, S. B.; Stys, P. K. *Nat. Med.* **2007**, *13*, 874–879.

(7) Skokos, D.; Shakhar, G.; Varma, R.; Waite, J. C.; Cameron, T. O.; Lindquist, R. L.; Schwickert, T.; Nussenzweig, M. C.; Dustin, M. L. *Nat. Immunol.* **2007**, *8*, 835–844.

(8) Kuchibhotla, K. V.; Lattarulo, C. R.; Hyman, B. T.; Bacskai, B. J. *Science* **2009**, *323*, 1211–1215.

(9) Canepari, M.; Mammano, F. *J. Neurosci. Methods* **1999**, *87*, 1–11.

(10) Eilers, J.; Callewaert, G.; Armstrong, C.; Konnerth, A. *Proc. Natl. Acad. Sci. U.S.A.* **1995**, *92*, 10272–10276.

(11) Leinekugel, X.; Medina, I.; Khalilov, I.; Ben-Ari, Y.; Khazipov, R. *Neuron* **1997**, *18*, 243–255.

(12) Mainen, Z. F.; Malinow, R.; Svoboda, K. *Nature* **1999**, *399*, 151–155.

(13) Kovalchuk, Y.; Eilers, J.; Lisman, J.; Konnerth, A. *J. Neurosci.* **2000**, *20*, 1791–1799.

(14) Losonczy, A.; Makara, J. K.; Magee, J. C. *Nature* **2008**, *452*, 436–441.

(15) Kao, J. P. Y.; Harootunian., A. T.; Tsien, R. Y. *J. Biol. Chem.* **1989**, *264*, 8179–8184.

(16) Yuste, R.; Katz, L. C. *Neuron* **1991**, *6*, 333–344.

(17) Smetters, D.; Majewska, A.; Yuste, R. *Methods* **1999**, *18*, 215–221.

(18) Peterlin, Z. A.; Kozloski, J.; Mao, B.-Q.; Tsiola, A.; Yuste, R. *Proc. Natl. Acad. Sci. U.S.A.* **2000**, *97*, 3619–3624.

(19) Mao, B.-Q.; Hamzei-Sichani, F.; Aronov, D.; Froemke, R. C.; Yuste, R. *Neuron* **2001**, *32*, 883–898.

(20) Cossart, R.; Aronov, D.; Yuste, R. *Nature* **2003**, *423*, 283–288.

(21) Ikegaya, Y.; Aaron, G.; Cossart, R.; Aronov, D.; Lampl, I.; Ferster, D.; Yuste, R. *Science* **2004**, *304*, 559–564.

(22) *The Molecular Probes® Handbook: A Guide to Fluorescent Probes and Labeling Technologies*, 11th ed.; Johnson, I., Spence, M. T. Z., Eds.; Invitrogen Corp.: Carlsbad, CA, 2010.

(23) Weissleder, R. *Nat. Biotechnol.* **2001**, *19*, 316–317.

(24) Kiyose, K.; Aizawa, S.; Sasaki, E.; Kojima, H.; Hanaoka, K.; Terai, T.; Urano, Y.; Nagano, T. *Chem.—Eur. J.* **2009**, *15*, 9191–9200.

(25) Tsien, R. Y. Monitoring Cell Calcium. In *Calcium as a Cellular Regulator*; E. Carafoli and C. Klee Eds. Oxford University Press: New York, 1999; pp 28−54.

(26) Ozmen, B.; Akkaya, E. U. *Tetrahedron Lett.* **2000**, *41*, 9185–9188.

(27) Koide, Y.; Urano, Y.; Hanaoka, K.; Terai, T.; Nagano, T. *ACS Chem. Biol.* **2011**, *6*, 600–608.

(28) Koide, Y.; Urano, Y.; Hanaoka, K.; Terai, T.; Nagano, T. *J. Am. Chem. Soc.* **2011**, *133*, 5680–5682.

(29) Fu, M.; Xiao, Y.; Qian, X.; Zhao, D.; Xu, Y. *Chem. Commun.* **2008**, 1780–1782.

(30) Nimmerjahn, A.; Kirchhoff, F.; Kerr, J. N. D.; Helmchen, F. *Nat. Methods* **2004**, *1*, 1–7.